IJERT
ISSN : 2278 - 0181

THESIS

Thesis ID : IJERTTH0003

A New Nonlinear Circuit To Identify Plasma Instabilities

Concetta Barcellona

UNIVERSITY OF CATANIA
CATANIA, ITALY

Published By

International Journal of Engineering Research and Technology
(www.ijert.org)

ISSN: 2278-0181

UNIVERSITY OF CATANIA

Department of Electrical, Electronics and System Engineering

Master's degree in Automation Engineering and Control of complex systems

Concetta Barcellona

A new nonlinear circuit to identify plasma instabilities

EXPERIMENTAL MASTER THESIS

Supervisor:
Prof. Luigi Fortuna
Eng. Arturo Buscarino
Eng. Claudia Corradino

ACADEMIC YEAR 2016/2017

Preface

In this work will be really considered the opportunity to model complex phenomena that have been discovered in Tokamak machine by using very simple analog nonlinear electronic circuits.
The possibility of using such a type of approach instead of using numerical models is due to have the opportunity to make various experiments in the circuit by changing the real parameters of the original model by using low cost resistor.
It is very useful from a qualitative point of view to have very simple circuits, but with very complex behavior that reflect exactly the original real system behavior. In this way a complete approach to study the dynamical behavior of the plasma can be easily performed with low cost electronic components.

Contents

List of Figures

LIST OF FIGURES

Introduction

In this work, a **low dimensional model** describing the quasi-periodic plasma dynamics observed in fusion experiments in Tokamaks [1] has been studied. This model is important for both a theoretical and a practical perspectives.
Oscillation of plasma's parameters (Edge Localized Nodes (ELMs), sawteeth) are observed when some large scale plasma instabilities do not lead to an immediate termination of a discarge resulting in periodic nonlinear perturbation of the plasma.
Understanding ELMs formation and development represents one of the main challenges in nuclear fusion research. In fact, these kind of instabilities can damage vessel wall components due to their extreme high energy transfer rate.
A low-dimensional description of ELMs dynamics is fundamental to qualitatively understand the effect of changes in the driving parameters (e.g. heating power) allowing to design dedicated control strategies (e.g. pellet injection for ELM mitigation).
Analyzing the main features of the plasma quantities, in particular when instabilities occur, could be helpful in order to control the overall reaction and to set up the confinement time.

The goal of this thesis has been to design and analyze the analogue circuital implementation of a well established minimal model of the main plasma instabilities. Thus, their complex dynamical behaviors has been investigated.

This thesis is organized in four chapters. Particularly, in the **first chapter** a low dimensional model of the spatiotemporal phenomena occurring in fusion plasma is described. An explanation of the model parameters and a description of the system dependance from these are reported. The different dynamical zones obtained by varying the parameters are also shown.

The **second chapter** deals with the circuit design and implementation. A detailed description on the circuit realization is provided focusing on the individual state variables and exploring the different behavioral regions taken into account in our work..

In the **third chapter**, the simulations perfomed by using Matlab®and the experimental results are shown. To validate the capabilities of the proposed model, a comparison with real measurements is discussed.

[1]A Tokamak is a magnetic confinement device developed to contain the hot plasma needed for producing controlled thermonuclear fusion power.

In the **fourth chapter**, a generalization of the model able to describes the pellet injection is performed. The pellet injection simulation, represented by the perturbation P(t), is performed by using the microcontroller board Arduino®Uno.

Chapter 1

Lower dimensional model of Plasma Instabilities

Nowaday, the growing energy consumption have led researchers to investigate novel alternative energy production. One of the most promising energy source is **nuclear fusion** that relies on the Einstein law for which the difference in mass between the products and reactants is converted into energy.
In the last decades, several nuclear devices have been designed in order to exploit nuclear fusion reactions able to generate energy.
The JET, Joint European Tokamak, is one of the Europe's largest fusion plants, located in Culham, United Kingdom. It is considered a fundamental test machine for the future reactor technology and plasma operating scenario.
The main goal of the nuclear fusion research is to overcome the issues related to the extreme operative conditions at which nuclear fusion reactions take place.

Figure 1.1: An internal view of the JET vessel with a complete metallic wall of beryllium and tungsten.

One of the main investigated configuration for the future nuclear fusion reactor is

the tokamak. It is a toroidal chamber where very high poloidal and toroidal magnetic fields confine plasma at high pressure and temperature.
The **magnetic confinement of fusion plasma**, operated by the tokamak [6] is fundamental in the process of nuclear fusion energy production. Usually, two main operative modes characterize nuclear fusion experiments depending on the adopted heating power needed to initiate nuclear fusion reactions inside the machine. Namely, the L-mode that is the low confinement regime and the H-mode that is the higher confinement regime. In fact, in the 1980's, it was discovery that by increasing the heating power over a threshold there is a bifurcation to a new state, named H-mode, due to the formation of insulating region at the plasma edge and also high profile gradients , such as pressure gradients.
These phenomena leads from one hand to an increase of the plasma magnetic confinement , from the other hand, to the occurance of instabilities, like the **Edge Localized Modes** (**ELMs**) [2].
ELMs are characterized by the emission of large amount of energy and particles, that hitting the surrounding vessel wall, may damage and even destroy it.
The objective of this work is to analyze and physically implement a **minimal model** that has been shown to be able to model the main plasma instabilities behaviours characterized by periodic non linear perturbation.
The knowledge of the main dynamical features of plasma quantities, in particular during instabilities, can be helpful in controlling their occurrecies and setting up the confinement time.
The model, introduced in [1], describes the interaction between a **relaxation process** and a **driving process**, occurring at diffent time-scale. Such a situation is encountered frequently in different processes taking place in plasma. The model is based on two plasma macroscopic quantities: the **amplitude of the displacement of the magnetic field** and the **plasma pressure gradient**.
Two equations are considered, the first one describes the **instability dynamics**, modeled as a relaxation phenomenon, where the displacement of the magnetic field from the equilibrium represents the variable of interest. The second equation illustrates the **power balance** dynamics, which drives the system towards the ELMs and models the pressure gradient behavior.[3]
The equations that describe the normalized dynamical systems are the following:

$$\begin{aligned} \ddot{\xi} &= (p-1)\xi - \delta\dot{\xi} \\ \dot{p} &= \eta(h - p - \beta\xi^2 z) \end{aligned} \tag{1.1}$$

where ξ is the amplitude of the displacement of the magnetic field, p is the plasma pressure gradient and δ, η, h and β are parameter of the system.
Introducing the variables $x = \dot{\xi}$, $y = k\xi$ and $z = p$, where k is a normalizing factor including the β parameter, the system 1.1 can be written in the form of a dimensionless system of three first order ordinary differential equations:

$$\boxed{\begin{aligned}\dot{x} &= (z-1)y - \delta x \\ \dot{y} &= x \\ \dot{z} &= \eta(h - z - y^2 z)\end{aligned}} \tag{1.2}$$

The model 1.2 qualitative describes the dependence of the system from three parameters, that determines its behavior:

- δ represents the **dissipation/relaxation** of perturbation related to ELMs burst;
- η represents **heat diffusion** coefficient;
- h is the **normalized power** input into the system and is responsible for inducing a burst.

A very important feature of the system is the capability of modeling plasma unstable nonlinear dynamics above a critical input power threshold (h>1). As a conseguence, by setting the input power as ***h*=1.5** and δ and η as indipendent parameters, it is possible to model several dynamical regimes as shown in Fig. 1.2:

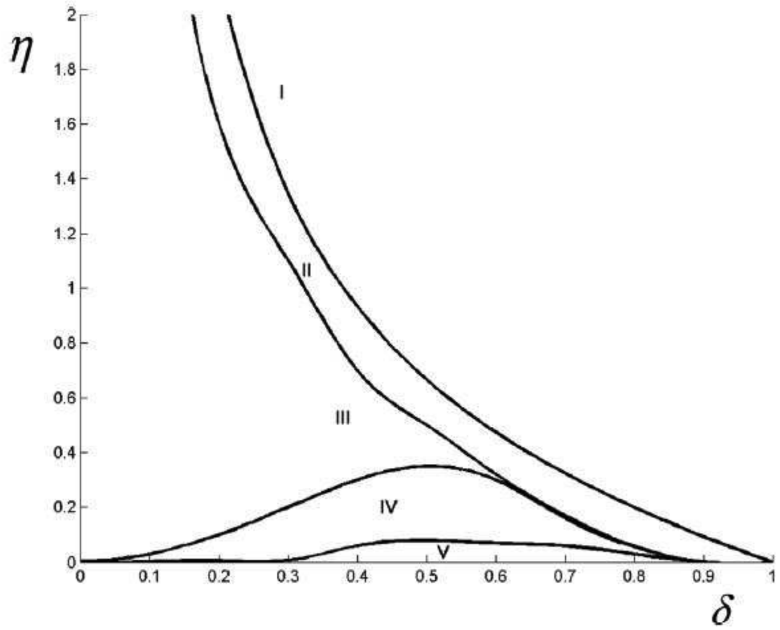

Figure 1.2: Dynamical regimes of oscillation for h=1.5.

The dynamical zones of oscillations in the (δ, η) plane are the following:

- zone I: **damped oscillation**;
- zone II and III: **periodic oscillations**, with simple and double periodicity respectively;

- zone IV: **chaotic oscillations**;
- zone V: **periodic orbits** for each (x_0,y_0,z_0) with $z_0 < 1$. For lower η values the oscillation are of **ELMs/sawtooth type**, characterized by slow-fast dynamics.

The Fig. 1.3 is a zoom of the different dynamical regions of oscillation.

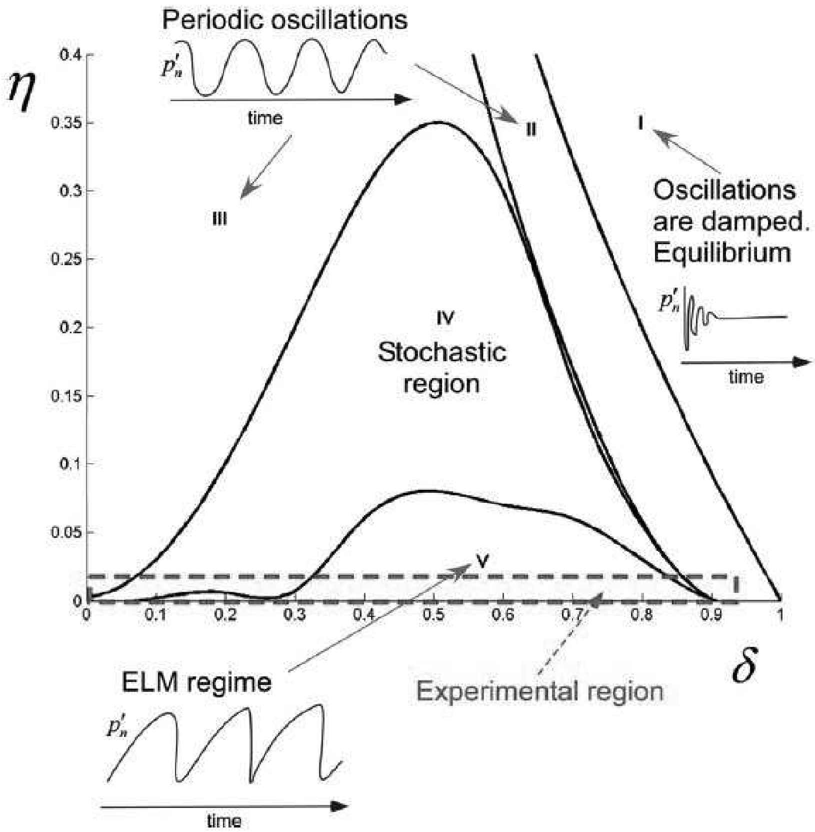

Figure 1.3: Zoom of dynamical zones of oscillation for h=1.5

In the third chapter, a deeper investigation of the system variables behaviors for each of these regions will be provided.

ISSN: 2278-0181

Chapter 2

Circuit analysis of low model Plasma instabilities

The physical realization of an ideal model represents a powerful tool to both verify the model ability to reproduce the theoretical dynamical behavior and investigate hidden dyamics due to intrinsic uncertainties introduced by real components.

The circuital design and implementation of the nonlinear model 1.2 has been performed in 2 steps by using off-the-shelf components.
Firstly, each single system equation has been analyzed and the related analogue circuit opportunely designed.
Secondly, all the designed sub-circuits have been gathered to build the entire one.

2.1 Main features of the circuit

In order to design a circuital analogue of a mathematical model the following components are required. Usually, the integration operation is performed by using an operational amplifier, i.e. quad **operational amplifiers** TL084IN.
The Fig. 2.1 shows the pin configuration and the functions of the amplifier.

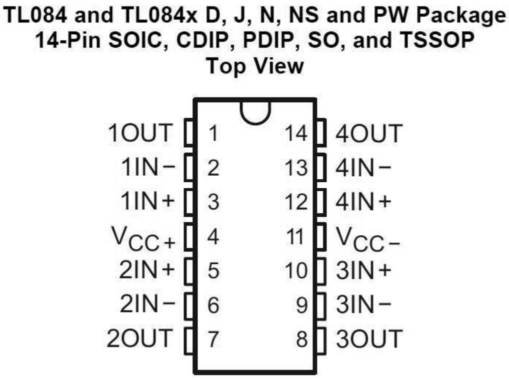

Figure 2.1: Pin configuration and functions of the TL084 operational amplifier.

The product can be realized by using an **analog multiplier**, i.e. the four quadrant AD633 for which the pin configuration is provided in Fig. 2.2.

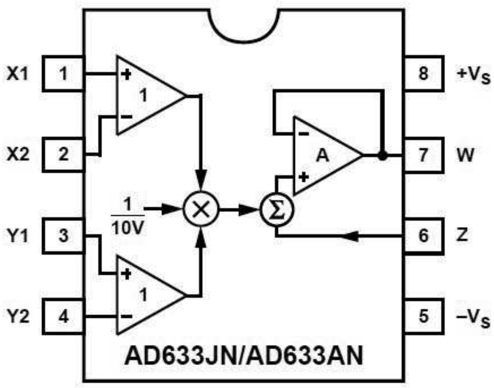

Figure 2.2: Pin configuration and block scheme of the AD633 analog multiplier.

The trasfer function of the multiplier is the following:

$$W = \frac{(X_1 - X_2)(Y_1 - Y_2)}{10V} + Z \tag{2.1}$$

where X and Y are differential inputs, Z in a high impedance summing input. The low impedance output voltage is a nominal 10V full scale provided by a buried Zener.
Both the AD633 and TL084 has been used in the circuital design of the plasma instabilities model 1.2, together with a **supply voltage** of $\pm 15V$.

The following nominal values for the system **parameters** are considered: $h = 1.5$, $\eta = 0.01$ and $\delta = 0.5$. η has been choosen as bifurcation parameter thus it has been implemented by using a potenziomenter spanning from min 0 to max 0.34. This allows to explore all the dynamical regimes of the system.

2.2 Circuit design for the x state variable

The first equation of the model 1.2 is the following:

$$\dot{x} = (z-1)y - \delta x = +zy - y - \delta x \tag{2.2}$$

Starting from this equation, the circuit in Fig. 2.3 can be retrieved.

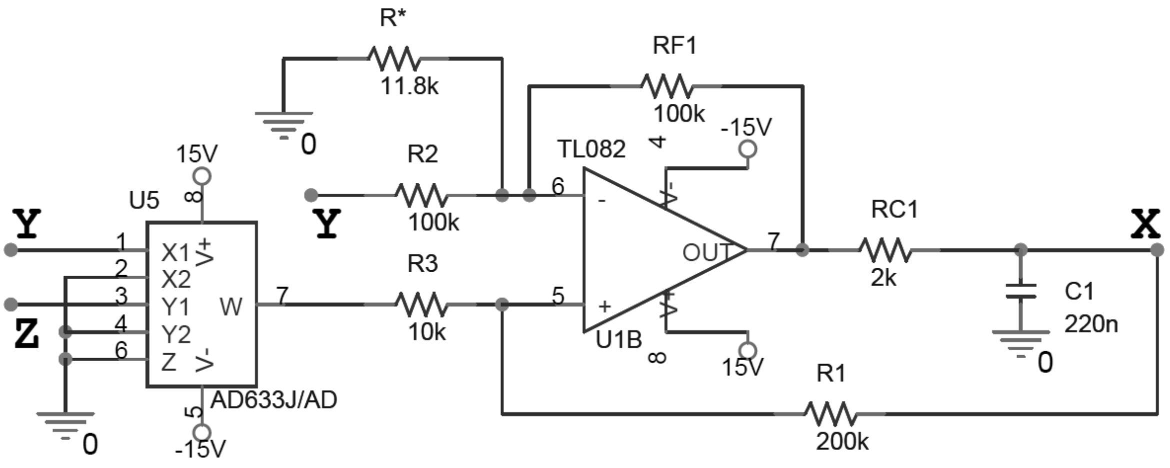

Figure 2.3: Scheme of the circuit associated to the x variable.

Let us fix $C_1 = 220nF$, $R_{C1} = 2k\Omega$ and $R_{F1} = 100k\Omega$.
It can be proved that the following formula can be derived [1]:

$$R_{C1}C_1\dot{x} = \frac{R_{F1}}{R_1}x - \frac{R_{F1}}{R_2}y + \frac{R_{F1}}{R_3}V^* - x$$

$$\dot{x} = \frac{1}{R_{C1}C_1}\left[\left(\frac{R_{F1}}{R_1} - 1\right)x - \frac{R_{F1}}{R_2}y + \frac{R_{F1}}{R_3}V^*\right] \tag{2.3}$$

More details on the utilized method can be found on the article: "A concise guide to chaotic electronic circuits"[4].

The value of each term is calculated:

$$\frac{R_{F1}}{R_1} - 1 = -\delta$$

$$R_1 = \frac{R_{F1}}{1-\delta} = \frac{100k\Omega}{1-0.5} = \frac{100k\Omega}{0.5} = 200k\Omega \tag{2.4}$$

[1] To find the formula 2.3 with an analytic method the current that flows on the capacitor is considered and chosen as state variables: $i_{C1} = C_1\frac{dV_1}{dt}$, $V_{C1} = x$, $i_{C1} = C_1\dot{x}$. Therefore it is possible to work on the circuit by substituting i_{C1} utilizing the different laws of electrotechnics. In this way the relationship between the circuit and the state variables is found.

$$-\frac{R_{F1}}{R_2} = -1$$

$$R_2 = R_{F1} = 100k\Omega \tag{2.5}$$

$$\frac{R_{F1}}{R_3}\frac{1}{10} = 1$$

$$R_3 = \frac{R_{F1}}{10} = \frac{100k\Omega}{10} = 10k\Omega \tag{2.6}$$

The next step is to verify that the **gain rule** is valid:

$$\sum\left(\frac{1}{R}\right)^{+} = \sum\left(\frac{1}{R}\right)^{-} \tag{2.7}$$

$$\frac{1}{R_1} + \frac{1}{R_3} = \frac{1}{R_{F1}} + \frac{1}{R_2} + \frac{1}{R^*} \tag{2.8}$$

where R^* is a compensation resistor that is added in the positive or negative pin of the amplificator if the relation is not verified.

$$\frac{1}{2R_{F1}} + \frac{10}{R_{F1}} = \frac{1}{R_{F1}} + \frac{1}{R_{F1}} + \frac{1}{R^*}$$

$$\frac{17}{2R_{F1}} = \frac{1}{R^*}$$

$$R^* = \frac{2R_{F1}}{17} = 11.8k\Omega \tag{2.9}$$

If a negative resistor value is obtained, the resistor must be connected with the other pin (this is due to the values of the terms of the state equations).

2.3 Circuit design for the y state variable

The same procedure described in section 2.2 has been performed in order to find the circuital analogue associated with the second state equation. The second state equation of the model 1.2 is the following:

$$\dot{y} = x \tag{2.10}$$

Starting from this equation, the circuit in Fig. 2.4 can be retrieved.

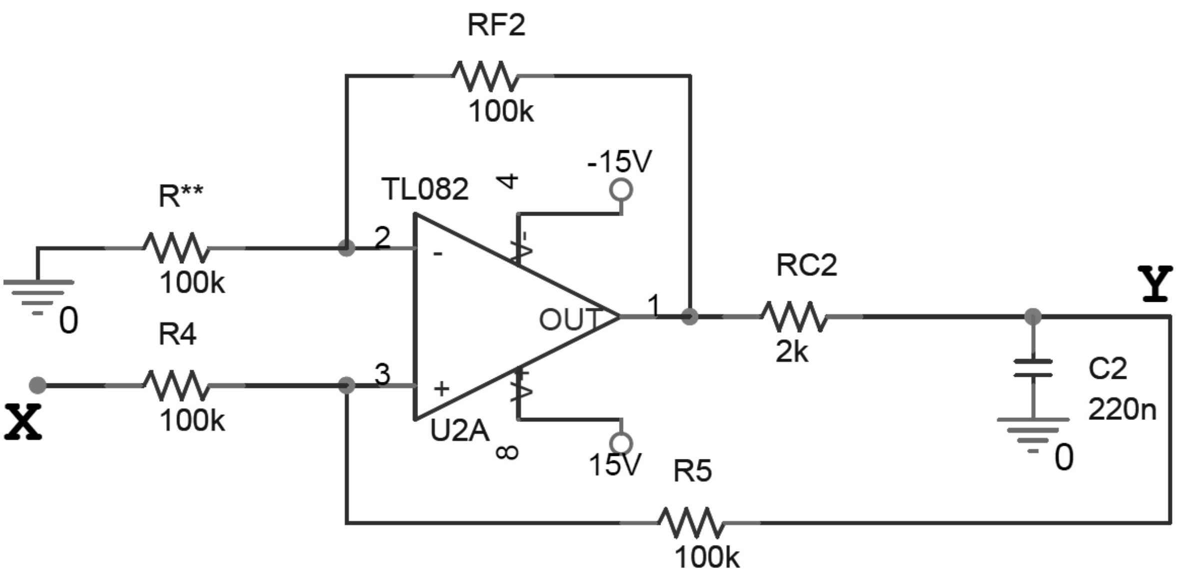

Figure 2.4: Scheme of the circuit associated to the y variable.

Let us fix $C_2 = 220nF$, $R_{C2} = 2k\Omega$ and $R_{F2} = 100k\Omega$. By making calculus it is possible to obtain the following expression:

$$R_{C2}C_2\dot{y} = \frac{R_{F2}}{R4}x + \left(\frac{R_{F2}}{R_5}y - y\right.$$

$$\dot{y} = \frac{1}{R_{C2}C_2}\left[\frac{R_{F2}}{R_4}x + \quad \frac{R_{F2}}{R_5} - 1\right)y\right] \tag{2.11}$$

Thereafter the value of each term is calculated:

$$\frac{R_{F2}}{R_4} = 1$$

$$R_4 = R_{F2} = 100k\Omega \tag{2.12}$$

$$\frac{R_{F2}}{R_5} - 1 = 0$$

$$R_5 = R_{F2} = 100k\Omega \tag{2.13}$$

The gain rule can be satisfy by using a compensation resistor R^{**}:

$$\sum\left(\frac{1}{R}\right)^{+} = \sum\left(\frac{1}{R}\right)^{-}$$

$$\frac{1}{R_4} + \frac{1}{R_5} = \frac{1}{R^{**}} + \frac{1}{R_{F2}} \tag{2.14}$$

$$R^{**} = R_{F2} = 100k\Omega \tag{2.15}$$

2.4 Circuit design for the z state variable

Even in the case of the third state equation design, the procedure described in section 2.2 has been adopted.
The expression of the third state equation is the following:

$$\dot{z} = \eta(h - z - y^2 z) \tag{2.16}$$

The circuit implemented is illustrated in Fig. 2.5:

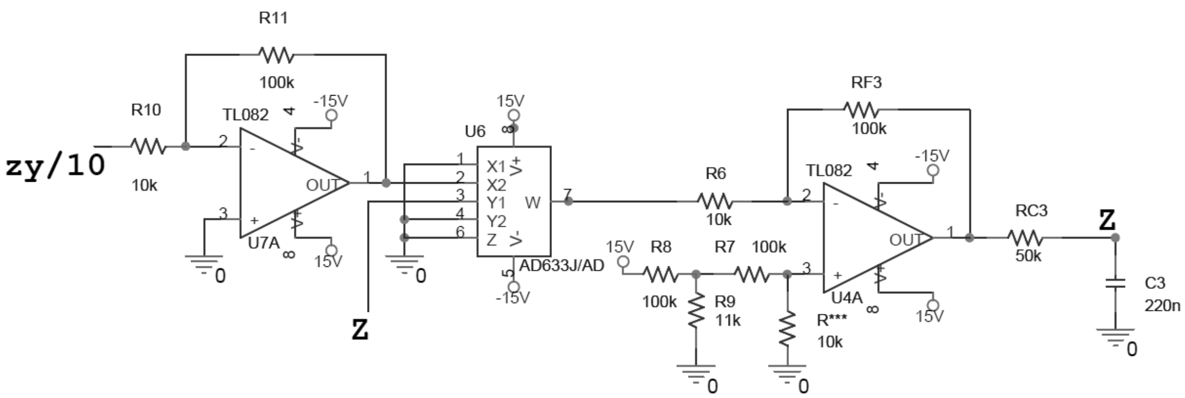

Figure 2.5: Scheme of the circuit associated to the z variable.

A **non inverting configuration operational amplifier** is connected between the output of the AD633 multiplier (implementing the zy product in 2.2) and the input of the third state variable circuit. Due to the fact that the AD6333 transfer function attenuates the output of a factor of $\frac{1}{10}$, an amplification stage of a factor of 10 is implemented. In particular, a gain of $G = \frac{R_{11}}{R_{10}} = \frac{100k}{10} = 10$ is obtained, thus achieving $-yz$ at the output , instead of $\frac{-yz}{10}$, in order to avoid to work with very low amplutude signals. The operational amplifier output is then connected with the X_2 pin of the multiplier in order to have a change of sign.

Let us fix $C_3 = 220nF$ and $R_{F3} = 100k\Omega$. The resistor R_{C3} was implemented with a **potentiometer** with nominal value of $100k\Omega$, in order to change the η value and find the behavior of the different dynamical regions. The relationship between the η parameter and the potentiometer is the following:

$$\eta = \frac{R_{C1}}{R_{C3}}$$

In this way the time constants of the three state variables are fixed at the same value. The expression of the dynamical evolution of the z variable is the following:

$$R_{C3}C_3\dot{z} = -\frac{R_{F3}}{R_6}V^{**} + \frac{R_{F3}}{R_7}V - z$$

$$\dot{z} = \frac{1}{R_{C_3}C_3}\left[\frac{R_{F3}}{R_7}V - z - \frac{R_{F3}}{R_6}V^{**}\right] \tag{2.17}$$

The value of each term of the equation can be find by comparison with the state equation 2.16:

$$\frac{R_{F3}}{R_7}V = h$$

$$R_7 = R_{F3} = 100k\Omega \tag{2.18}$$

in which V is fixed equal h, so $V = h = 1.5V$. In order to obtain 1.5V from the supply voltage of 15V a voltage divider is build with the resistors $R_8 = 100k\Omega$ and $R_9 = 11k\Omega$. The resistor value R_6 is found with the following relation:

$$-\frac{R_{F3}}{R_6}V^{**} = -y^2 z$$

$$R_6 = \frac{R_{F3}}{10} = 10k\Omega \tag{2.19}$$

where V^{**} is the output of the second multiplier and it is equal to:

$$V^{**} = \frac{y^2 z}{10}$$

Finally, the gain rule is verified by using a compensation resistor R^{***}:

$$\sum\left(\frac{1}{R}\right)^+ = \sum\left(\frac{1}{R}\right)^-$$

$$\frac{1}{R_7} + \frac{1}{R^{***}} = \frac{1}{R_6} + \frac{1}{R_{F3}} \tag{2.20}$$

$$R^{***} = R_6 = 10k\Omega \tag{2.21}$$

2.5 Overall circuit

The **equations** governing the circuit behavior are:

$$\begin{aligned}\dot{x} &= \frac{1}{R_{C1}C_1}\left[\left(\frac{R_{F1}}{R_1}-1\right)x-\frac{R_{F1}}{R_2}y+\frac{R_{F1}}{R_3}V^*\right]\\ \dot{y} &= \frac{1}{R_{C2}C_2}\left[\frac{R_{F2}}{R_4}x+\left(\frac{R_{F2}}{R_5}-1\right)y\right]\\ \dot{z} &= \frac{1}{R_{C3}C_3}\left[\frac{R_{F3}}{R_7}V-z-\frac{R_{F3}}{R_6}V^{**}\right]\end{aligned} \tag{2.22}$$

where:

$$V^*=\frac{zy}{10},\quad V=15V,\quad V^{**}=\frac{y^2z}{10}$$

Therefore the circuit parameters are chosen so that 2.22 matches 1.2. The **electrical scheme** is shown in Fig. 2.6.

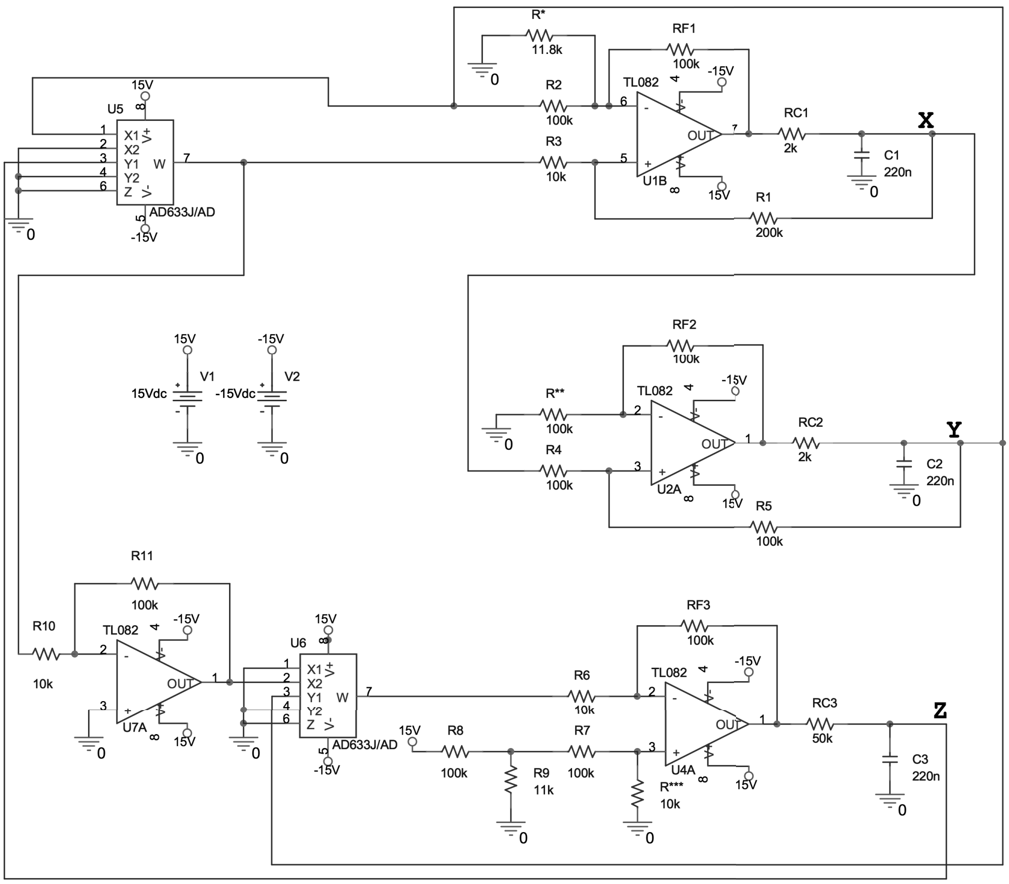

Figure 2.6: Scheme of the nonlinear circuit.

The Fig. 2.7 shows the circuit implemented in laboratory:

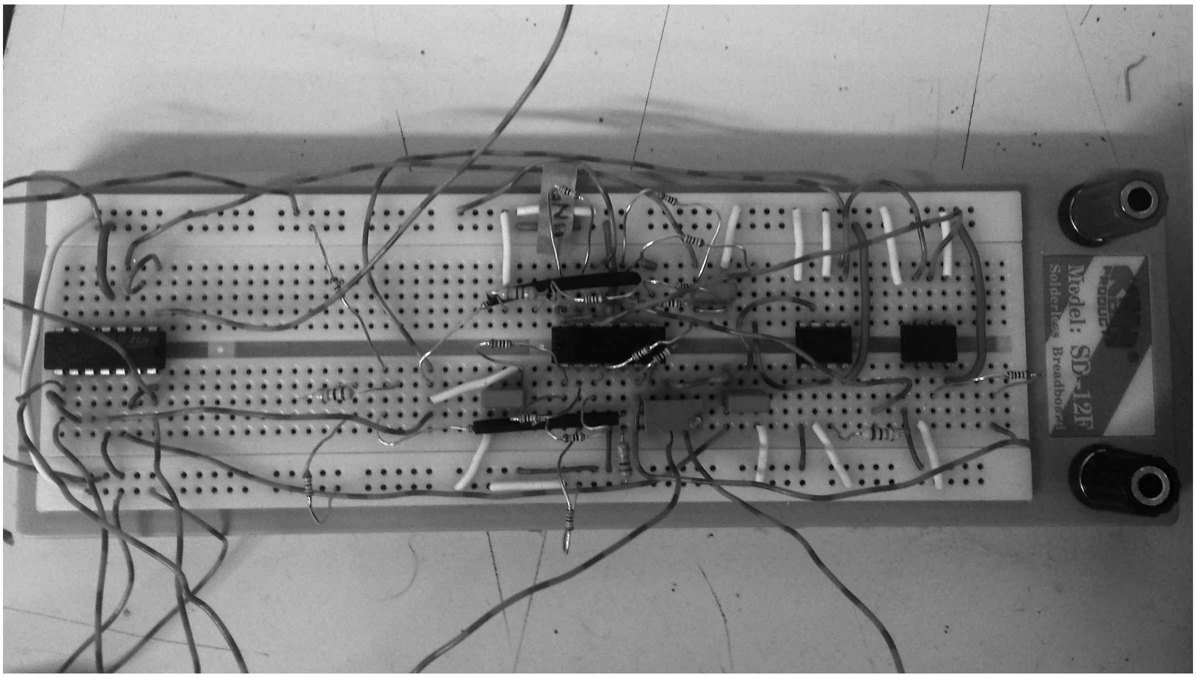

Figure 2.7: Implementation of the nonlinear circuit.

The signal acquisition is performed by using a National Instrument®data acquisition board. In the circuit implementation, an **operational amplifiar with a buffer connection** is added between the output of the circuit (x,y,z) and the board, in order to uncouple the circuit from the board.

Chapter 3

Bifurcation analysis and results

In this chapter, the simulations perfomed by using **Matlab®** and the experimental results will be shown. Signals were acquired using a **National Instrument®data acquisition board** with a sampling frequency $f_s = 50kHz$ and were elaborated using **LabVIEW®**.

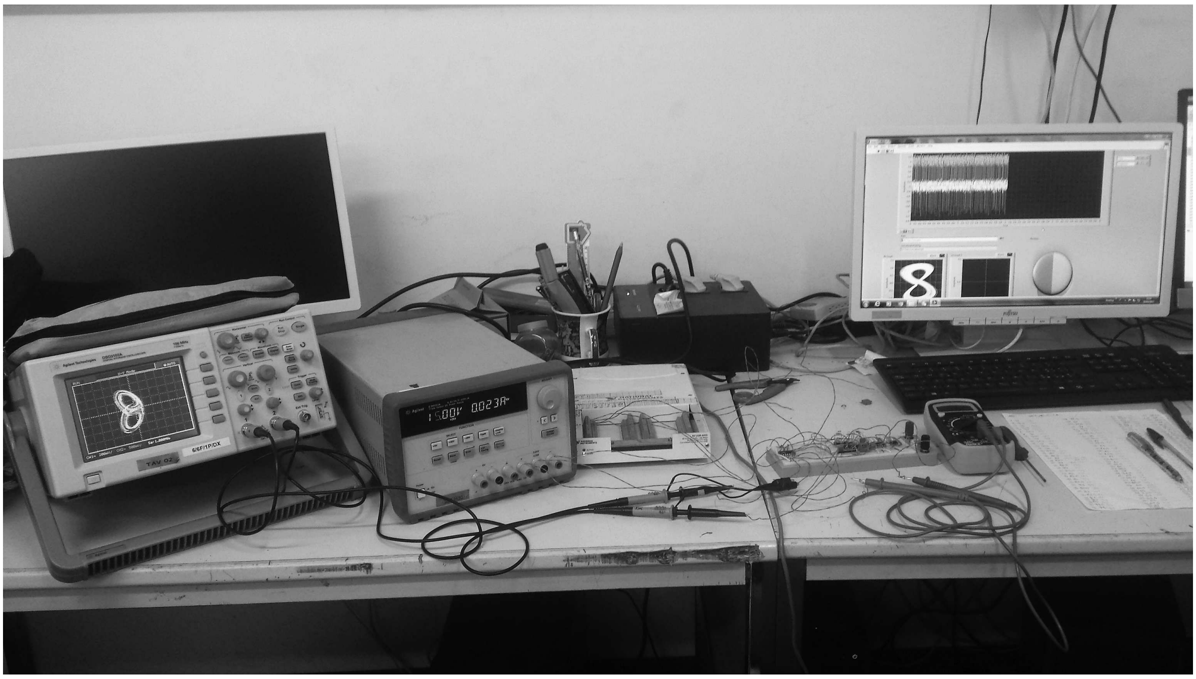

Figure 3.1: Overview of the data acquisition system used.

The circuit behavior, by varing η, was analyzed. In the Matlab®simulation we consider as initial conditions the values $(x_0, y_0, z_0) = (0; 1.70; 1.01)$.

ISSN: 2278-0181

3.1 Damped oscillations

The zone I, as reported in Fig. 1.2, is characterized by damped oscillations. The following pictures 3.2 show the results of Matlab®simulations:

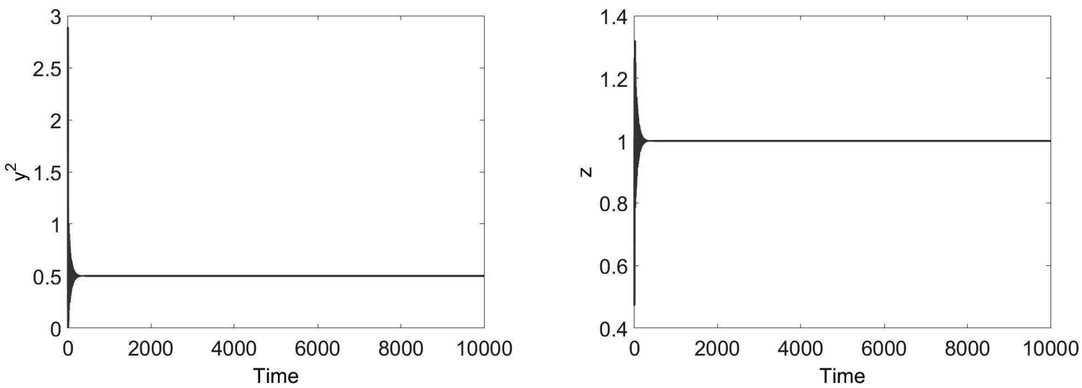

(a) *Function* $y^2(t)$ (b) *Function* $z(t)$

Figure 3.2: Simulations of damped oscillations in the case $(\delta, \eta) = (0.5; 0.668)$.

The results of the simulations are compared with the plot obtained in the oscilloscope:

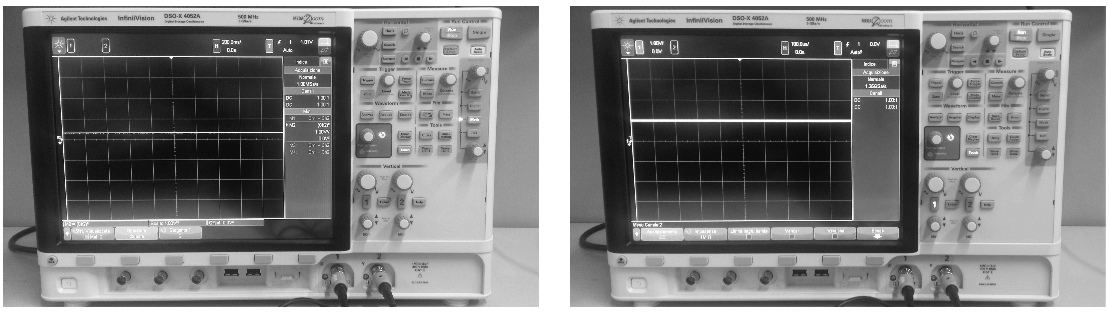

(a) *Function* $y^2(t)$ (b) *Function* $z(t)$

Figure 3.3: Oscilloscope traces of damped oscillations in the case $(\delta, \eta) = (0.5; 0.668)$.

CHAPTER 3. BIFURCATION ANALYSIS AND RESULTS

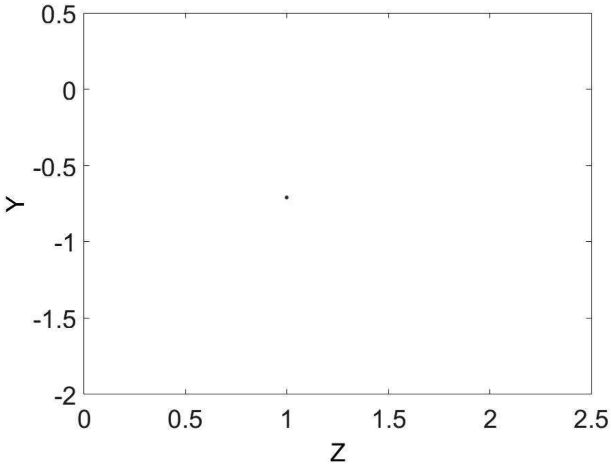

Figure 3.4: Attractor on the yz-plane in the case of damped oscillations $(\delta, \eta) = (0.5; 0.668)$.

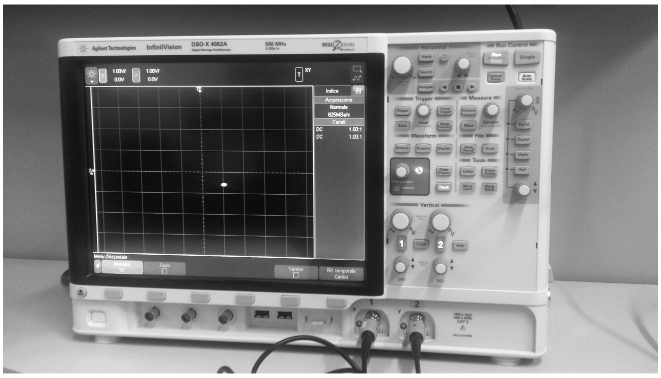

Figure 3.5: Oscilloscope trace of the attractor on the yz-plane in the case of damped oscillations $(\delta, \eta) = (0.5; 0.668)$.

3.2 Periodic oscillations

The zone II, as reported in Fig. 1.2, is characterized by simple periodic oscillations. The following picture 3.6 shows the results of Matlab®simulations:

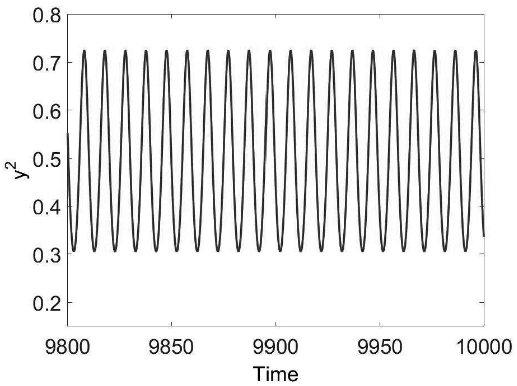

(a) *Function* $y^2(t)$

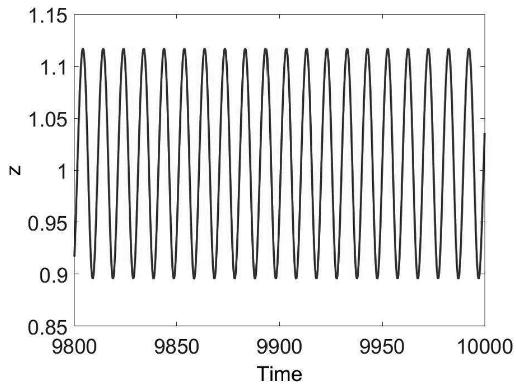

(b) *Function* $z(t)$

Figure 3.6: Simulations of periodic oscillations in the case $(\delta, \eta) = (0.5; 0.55)$.

The results of the simulations are compared with the plot obtained in the oscilloscope:

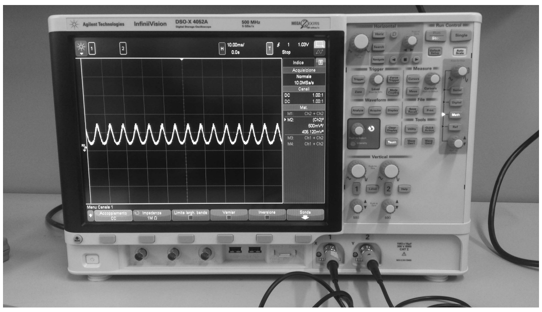

(a) *Function* $y^2(t)$

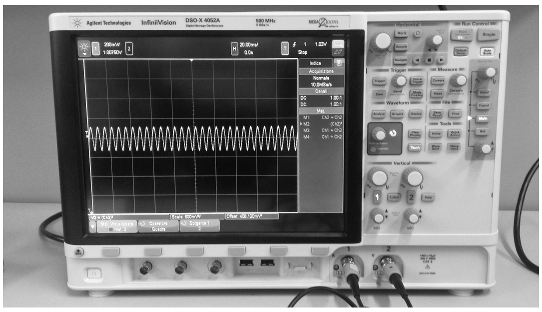

(b) *Function* $z(t)$

Figure 3.7: Oscilloscope traces of periodic oscillations in the case $(\delta, \eta) = (0.5; 0.55)$.

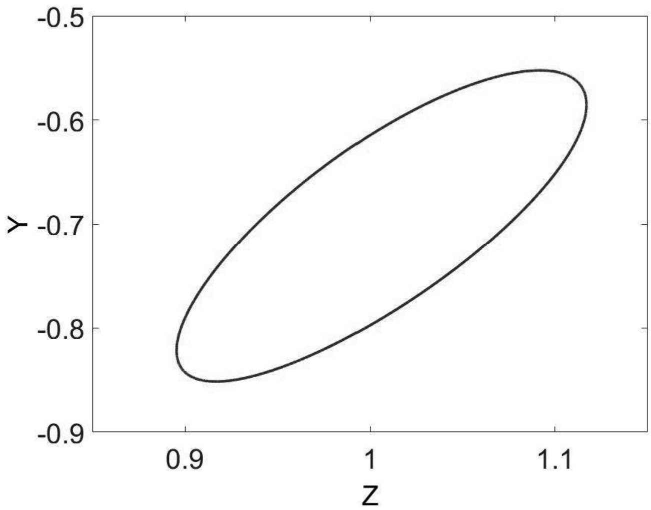

Figure 3.8: Attractor on the yz-plane in the case of periodic oscillations $(\delta, \eta) = (0.5; 0.55)$.

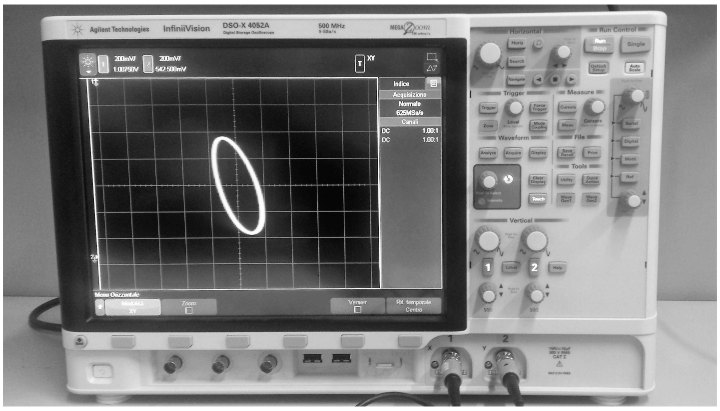

Figure 3.9: Oscilloscope trace of the attractor on the yz-plane in the case of periodic oscillations $(\delta, \eta) = (0.5; 0.55)$.

3.3 Chaotic oscillations

In zone IV chaotic oscillations occur. The following pictures 3.10 show the results of Matlab®simulations:

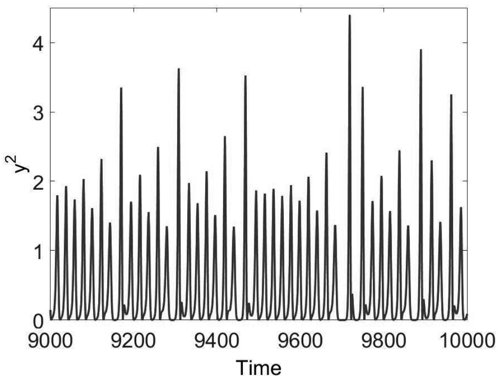

(a) *Function* $y^2(t)$

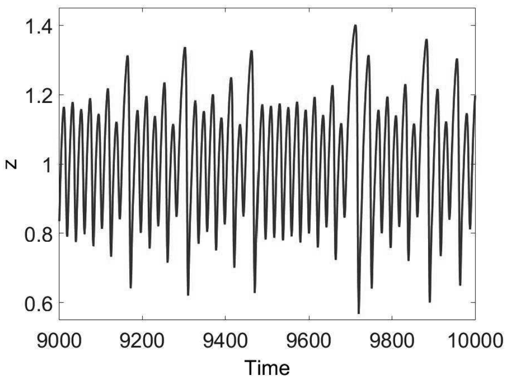

(b) *Function* $z(t)$

Figure 3.10: Simulations of chaotic oscillations in the case $(\delta, \eta) = (0.5; 0.08)$.

The results of the simulation are compared with the plot obtained in the oscilloscope:

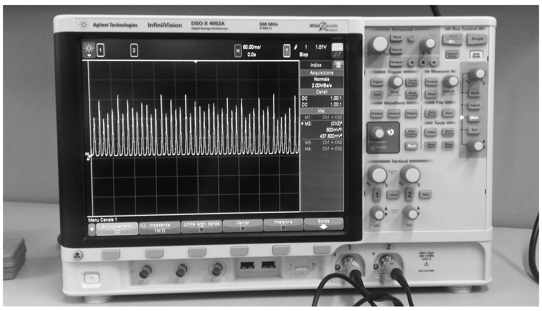

(a) *Function* $y^2(t)$

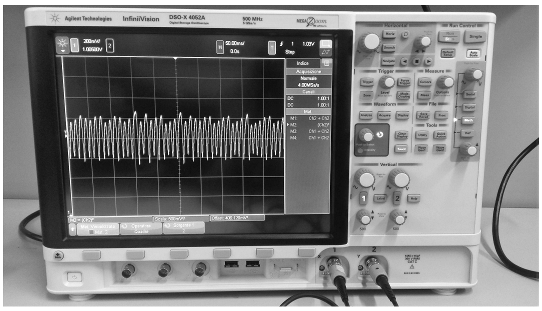

(b) *Function* $z(t)$

Figure 3.11: Oscilloscope traces of chaotic oscillations in the case $(\delta, \eta) = (0.5; 0.08)$.

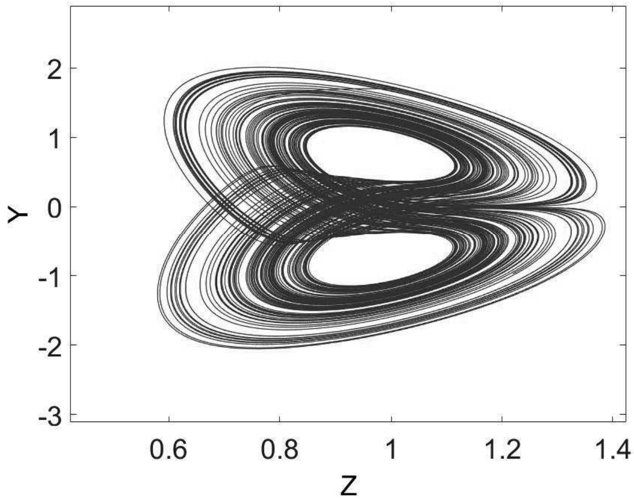

Figure 3.12: Attractor on the yz-plane in the case of chaotic oscillations $(\delta, \eta) = (0.5; 0.08)$.

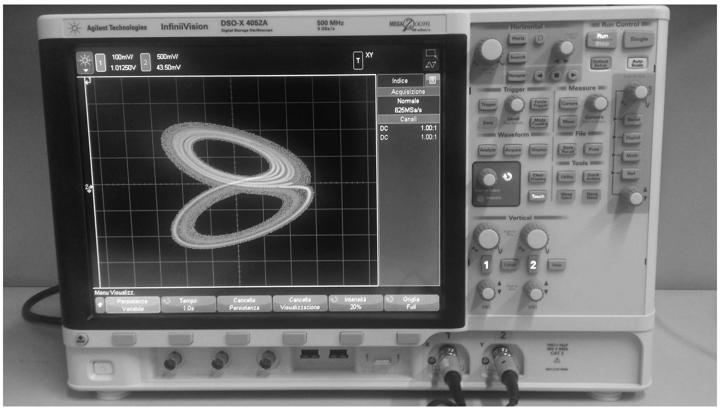

Figure 3.13: Oscilloscope trace of the attractor on the yz-plane in the case of chaotic oscillations $(\delta, \eta) = (0.5; 0.08)$.

3.4 ELM

In zone V oscillations of ELM/sawtooth type are observed when η decrease. The following pictures 3.14 show the results of Matlab®simulations:

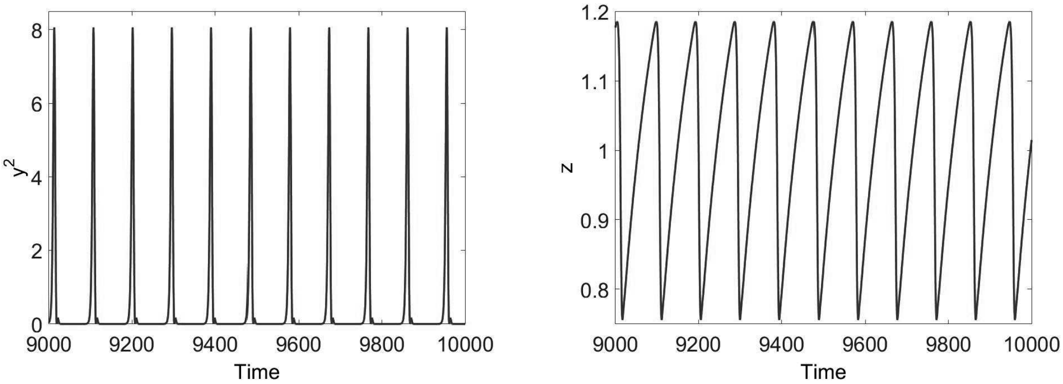

(a) *Function* $y^2(t)$ (b) *Function* $z(t)$

Figure 3.14: Simulations of ELM/sawtooth oscillations in the case $(\delta, \eta) = (0.5; 0.011)$.

The results of the simulation are compared with the plot obtained in the oscilloscope:

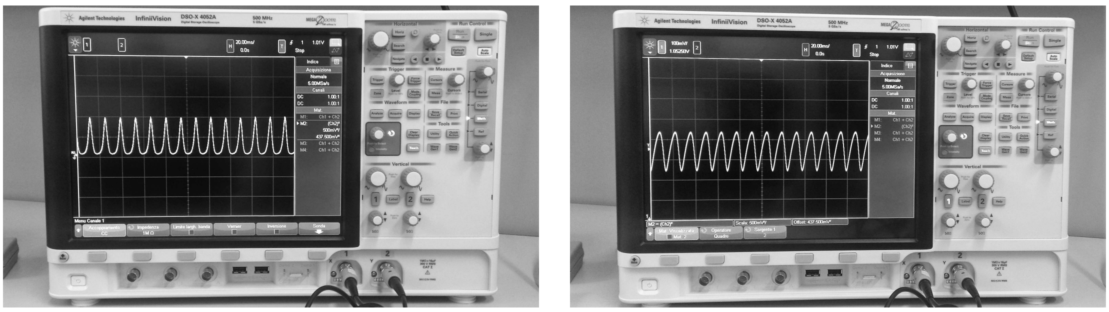

(a) *Function* $y^2(t)$ (b) *Function* $z(t)$

Figure 3.15: Oscilloscope traces of ELM/sawtooth oscillations in the case $(\delta, \eta) = (0.5; 0.01)$.

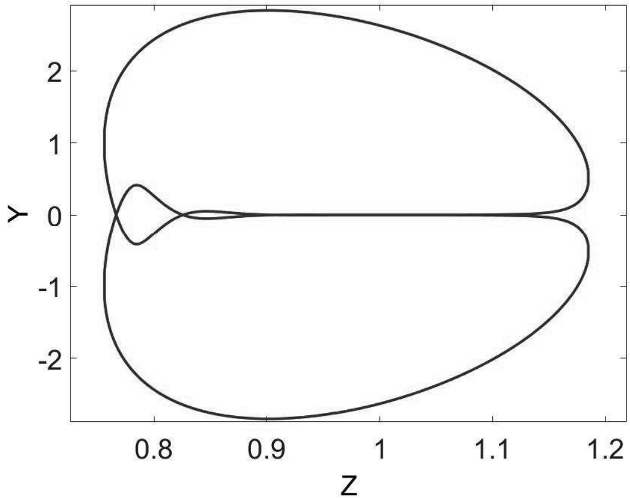

Figure 3.16: Attractor on the yz-plane in the case of ELM/sawtooth oscillations $(\delta, \eta) = (0.5; 0.01)$.

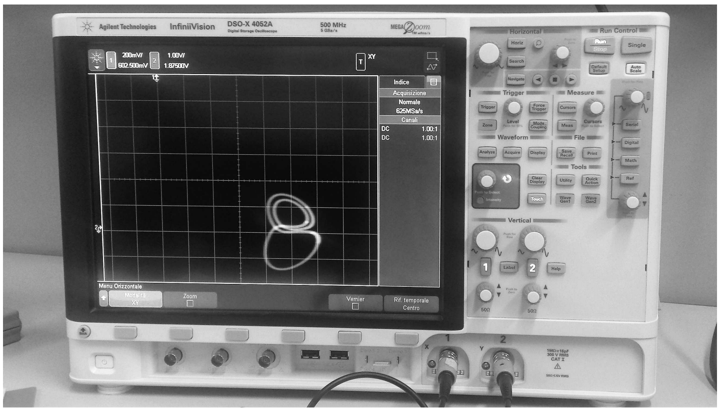

Figure 3.17: Oscilloscope trace of the attractor on the yz-plane in the case of ELM/-sawtooth oscillations $(\delta, \eta) = (0.5; 0.01)$.

3.5 Bifurcation diagrams

In the figures below, the bifurcation diagram [5] of the system is showed. In the first image 3.18 the diagram is obtained by using the ideal model.

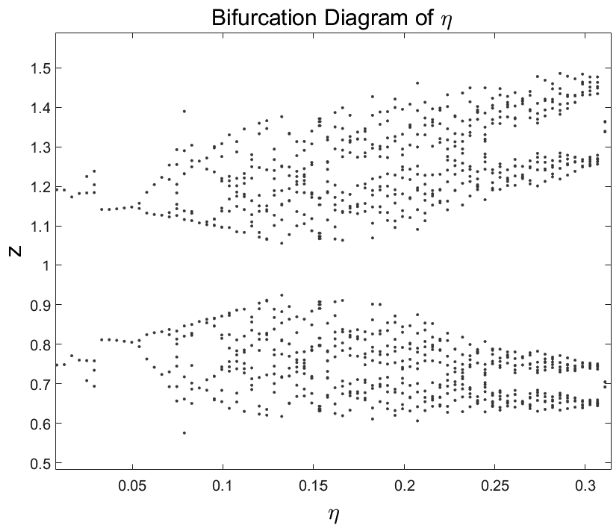

Figure 3.18: Bifurcation diagram of system 1.2 with respect to the bifurcation parameter η.

The plot 3.19 shows the bifurcation diagram obtained by using experimental data acquisitions.

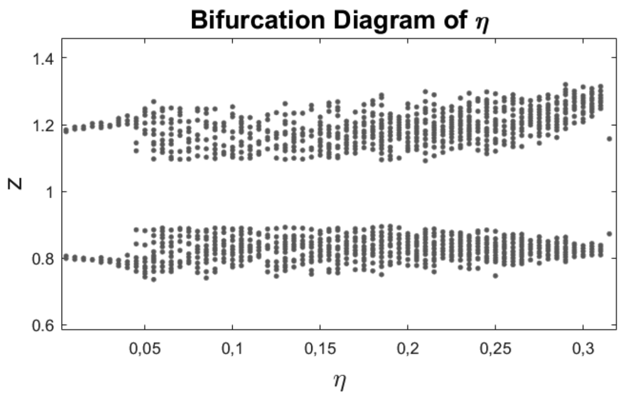

Figure 3.19: Experimental bifurcation diagram with respect to the parameter η.

Chapter 4

Pellet injection

In this chapter the model 1.2 is generalized in order to analyze the case of pellet injection into the plasma. The pellet injection is simulated by mean of the microcontroller board Arduino®Uno. This experiment relies on simple components and on a easy to use and low cost microcontroller board.

4.1 The model

The pellet injection into the plasma can mitigate the **ELMs** [1]. The modelling of such working condition is considered in [1] where a perturbation term is added in the first equation of the model 1.2:

$$\boxed{\begin{aligned} \dot{x} &= -\{1 - [z + P(t)]\}y - \delta x \\ \dot{y} &= x \\ \dot{z} &= \eta[h - zy^2 z] \end{aligned}} \tag{4.1}$$

The **perturbation P(t)** simulates the pellet injection and can be selected in the form :

$$P(t) = a * exp\{-[t - t_{period}\ int(t/t_{period}) - \delta_P]^2/b\} \tag{4.2}$$

where a is the perturbation amplitude, t_{period} is the perturbation period, δ_P is the perturbation shift and b is the perturbation width. The symbol "int" specify that the ratio must be integer.
The system parameters are set to work in the ELMs region: $h = 1.5$, $\delta = 0.5$, $\eta = 0.009$. Instead the perturbation parameters are chosen in the following way: $a = 5$, $t_{period} = 5$, $\delta_P = 2$ and $b = 2$.

4.2 Perturbation implementation by using Arduino®

The perturbation P(t) is generated by using the microcontroller board Arduino®Uno [7].

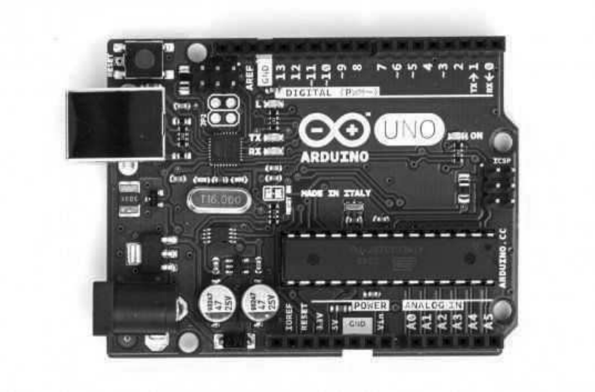

Figure 4.1: Microcontroller board Arduino®Uno.

The platform UNO is a robust multipurpose board, the most used and documented board of the whole Arduino®family. It can be used for coding and for work with electronics.
Arduino®Uno is based on the microcontroller ATmega328P. It has:

- **6 analog inputs**, that can be used with the function *analogRead()*;
- **Pins GND and 5V** give ground and 5V power to the circuit;
- **14 digital input/output pins**, utilized with the functions *digitalRead()*, *digitalWrite* and *analogWrite*. The latter only works on the pins with the symbol PWM;
- a **16 MHz quartz crystal**;
- a **USB connection**, used to power Arduino®Uno, to load the sketch in the board and to communicate with Arduino®through *Serial.println()*;
- a **power jack** used to power Arduino®when it is not connected with a USB port, can be used voltage between 7 and 12V;
- a **reset button**, that starts again the microcontroller ATmega;
- **ICSP header**;
- the **LED TX and RX** show the communication between Arduino®and the computer (can be useful during the debug);
- the **LED of the pin 13** is the only integrated actuator in Arduino Uno;
- the **Power LED ON** indicates that Arduino®is getting power.

The Arduino®Uno is fully programmable via an integrated development environment in C/C++.
The microcontroller is programmed so that the perturbation is implemented and the

result coded as an **8-bit word** and sent to the circuit by means of the digital output of the board. The digital signals are before converted to analog voltage through a **R-2R converter** [8].
The pin between 2 and 9 of the Arduino board are the output eight digits of the 8-bit word. The electrical scheme of the R-2R converter is shown in Fig. 4.2:

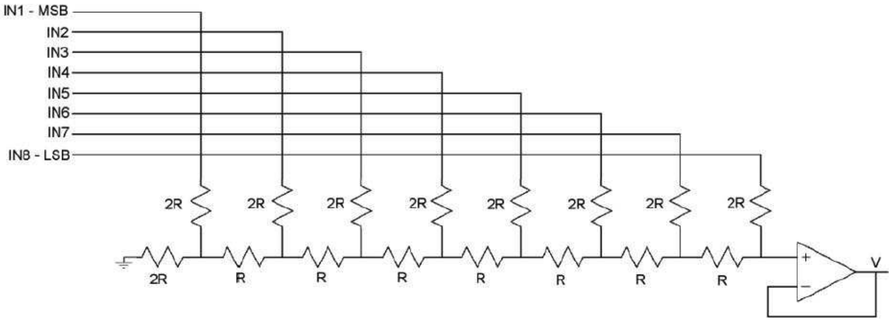

Figure 4.2: Electrical scheme of the R-2R converter.

The digital to analog converter is implemented utilizing a R-2R converter with an output buffer. R is equal $10k\Omega$ and the buffer is an operational amplifier TL084. The power supply is a dual voltage equal to $\pm 15V$. In the scheme 4.2 the signal of the pin 2 (that is the Most Significant Bit) is connected with the first resistor 2R on the left, the other connections are done consequently.

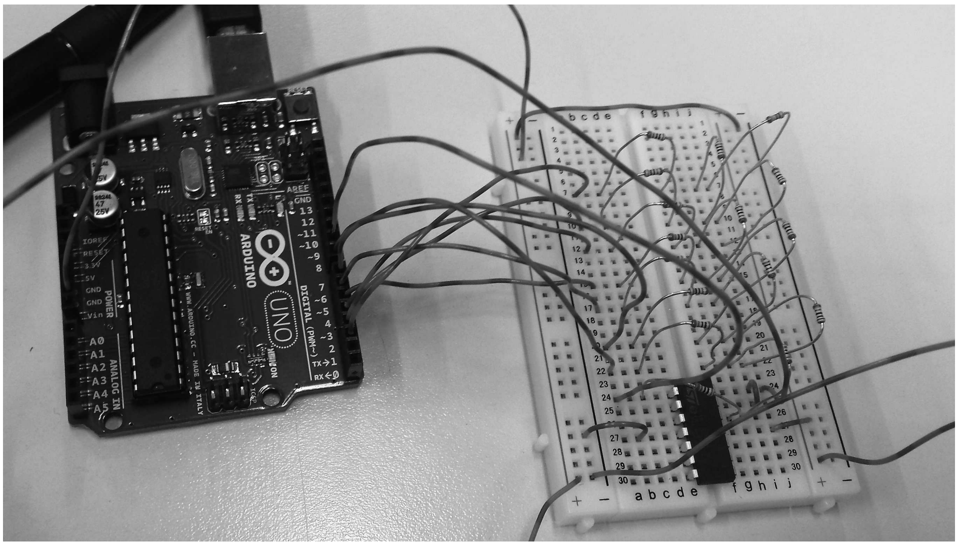

Figure 4.3: Complete setup of the pellet injection microcontroller implementation, utilizing the Arduino®board and the converter R-2R realized on the breadboard.

ISSN: 2278-0181

In the following the code utilized to generate the perturbation signal P(t):

```
/* Sketch: implementation of the perturbation P(t), that
simulates the pellet injection into the plasma.*/

float pert[150];  // 150 is the samples number
float P[150];
float pHigh=0;
int val;
float norm;
int j=0;

void setup() {
for(int pinNumber=2; pinNumber<10; pinNumber ++){
pinMode(pinNumber,OUTPUT); // set pin between 2 and 9 as output
}
}

void loop() {
if (j<1){
j=2;
for (int i=0; i<150; i++){
P[i]=5*exp(-(pow( (i) -150 *int ((i)/150) -2 ,2))/(1));

if (P[i]> pHigh){
pHigh=P[i];
}
}
}
norm=255/pHigh;

for (int i=0; i<150; i++){
pert[i]=P[i]*norm; /* Vector values normalization
between 0 and 255. */
val=pert[i];

for(int pinNumber=2; pinNumber<10; pinNumber++){
digitalWrite(pinNumber, val%2);
val=val/2;
}
}
delay(100);
}
```

In the first part of the sketch there is the variables declaration, in which the type variables

are specify (such as int, float).
In the second part the function **setup()** runs only one time after the Arduino board is turned on. Inside this the function **pinMode()** configures the digital pin between 2 and 9 as Output.
The third part is characterized by the function **loop**, that runs continuously after the execution of the setup(). In the first iteration the perturbation P(t) is generated and stored in the vector P[i]. Then the variable j is set equal 2, so through the if control this procedure is not repeated in the successive loop. In the next step the vector values are normalized in the range between 0 and 255. Finally the 8-bit digital expression is written on the output digital pin and send to the digital to analog converter.

4.3 Circuit design

In the circuit implementation, the **x block** is designed in agreement with the model 4.1:

$$\dot{x} = -\{1 - [z + P(t)]\}y - \delta x = -y + zy + P(t)y - \delta x$$

The perturbation term is implemented with an AD633 multiplier, the electrical scheme is shown in Fig. 4.4:

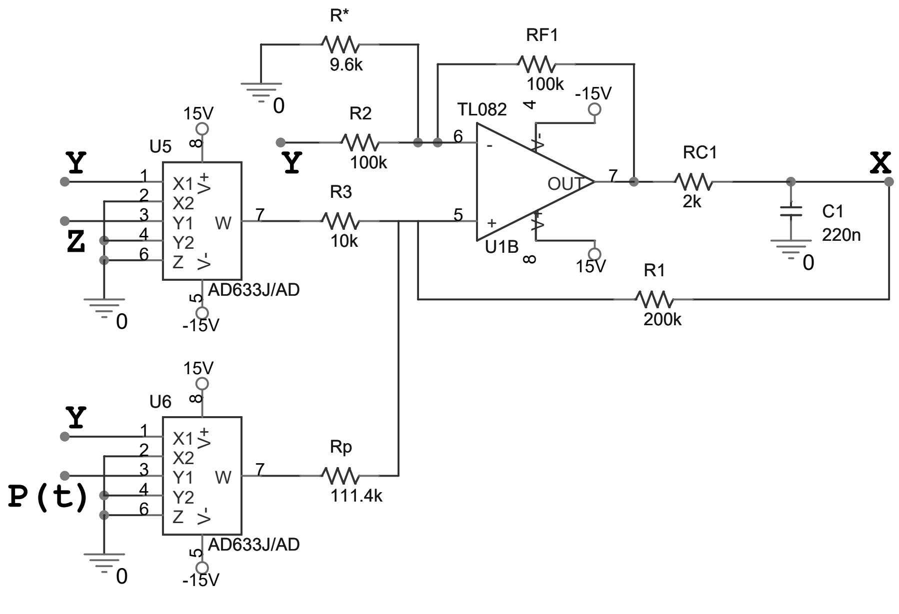

Figure 4.4: Circuit scheme of the x variable with the perturbation P(t).

Unlike the previous x block implementation, in this case the compensation resistor R^* has a different value equal to $9.6k\Omega$ and the resistor R_p is added in order to compensate the term 1/10 introduced from the multiplier and in order to normalized the perturbation

signal that has maximum value equal 5V. In order to have comparable frequencies with the perturbation the capacitor values used in the circuit are set in the following way: $C_1 = C_2 = C_3 = 10nF$.
The circuit implemented is shown in Fig. 4.5:

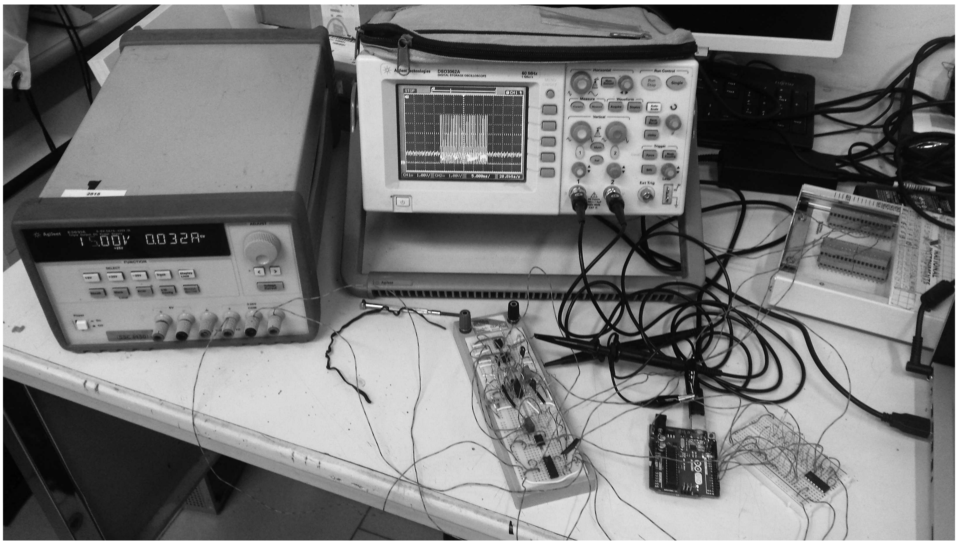

Figure 4.5: Circuit implementation in the case of Pellet injection.

Thesis - 2017 International Journal of Engineering Research & Technology (IJERT)
ISSN: 2278-0181

4.4 Results

In this section the data acquired by using the **National Instrument®data acquisition board** are shown. The sampling frequency is equal to $f_s = 150kHz$, because the signals are faster then the ones in the previous case. Thereafter the signals were elaborated in **LabVIEW®** and the simulation are done by using **Matlab®**.

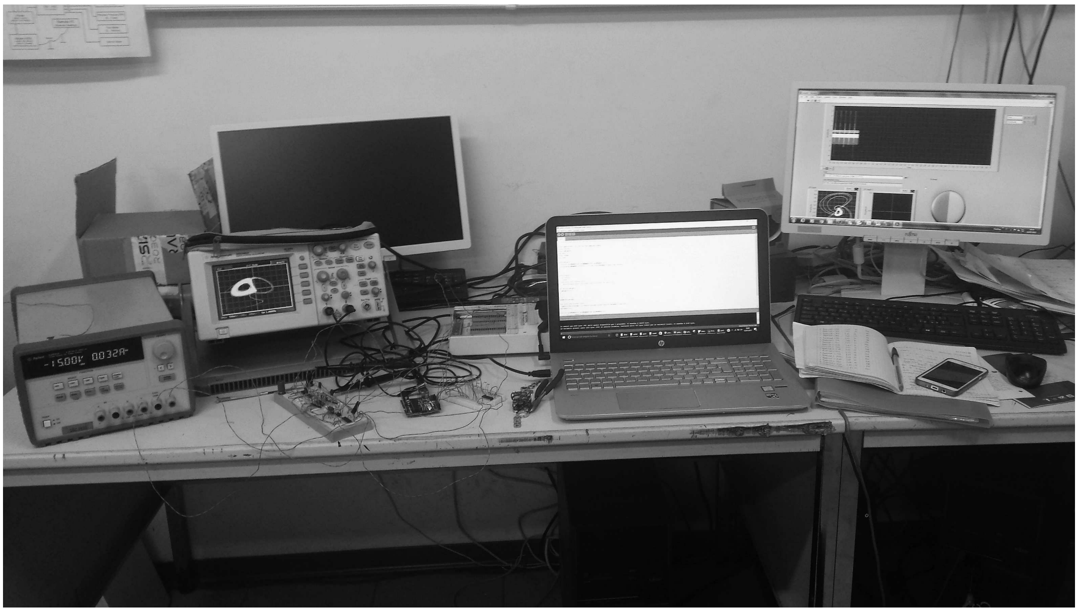

Figure 4.6: Data acquisition systems in the case of pellet injection.

CHAPTER 4. PELLET INJECTION

In the following pictures we can see a comparison between the plots obtained in the oscilloscope and the Matlab simulations performed with the data acquired. The picture 4.7 shows the behaviour of the z variable **before the pellet injection**:

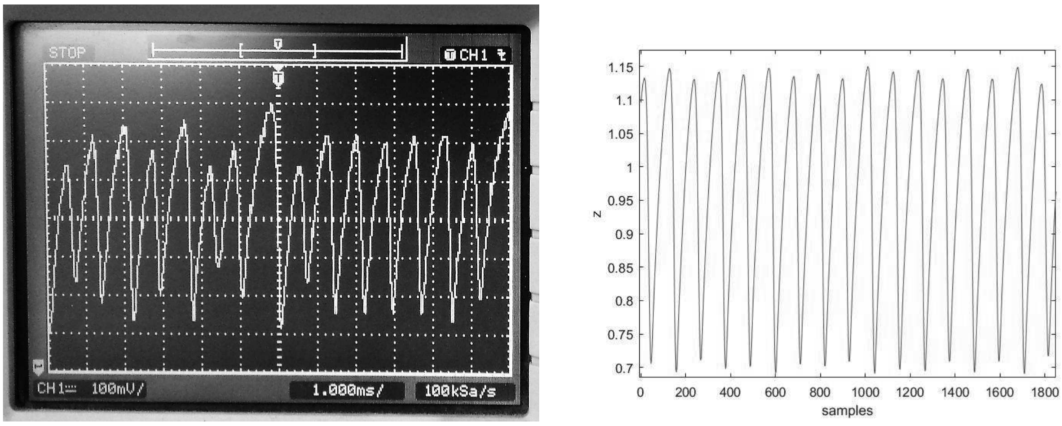

(a) *Oscilloscope trace* (b) *Acquired waveform*

Figure 4.7: Experimental trend of z variable before pellet injection.

In the Fig. 4.8 is shown the z behaviour in the **case of pellet injection**:

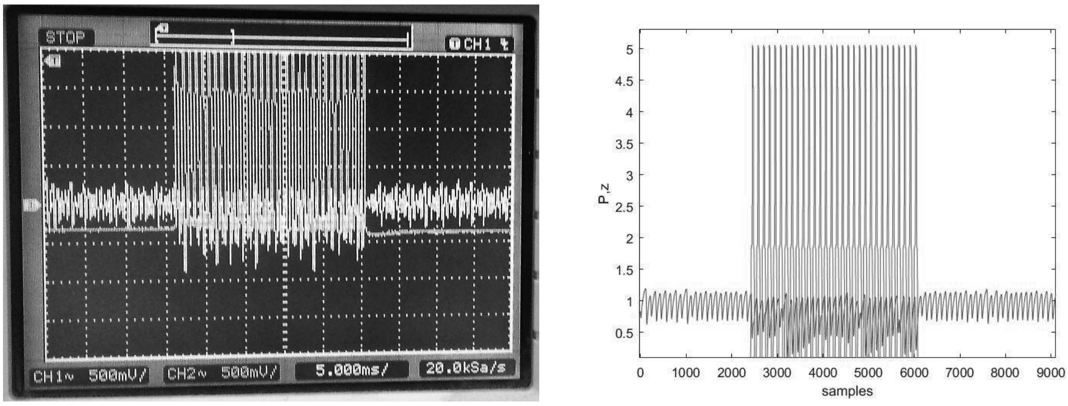

(a) *Oscilloscope trace* (b) *Acquired waveform*

Figure 4.8: Experimental trend of ELMs with pellet injection. Perturbations P(t) are shown by green lines in the case (a) and by red lines in the case (b).

By analyzing the result shown in Fig. 4.8 is possible to say that the perturbation changes the plasma stability and increases the ELMs frequency.

The Fig. 4.9 and Fig. 4.10 shows a comparison between the **attractors** in the case before the pellet injection and after the pellet injection.

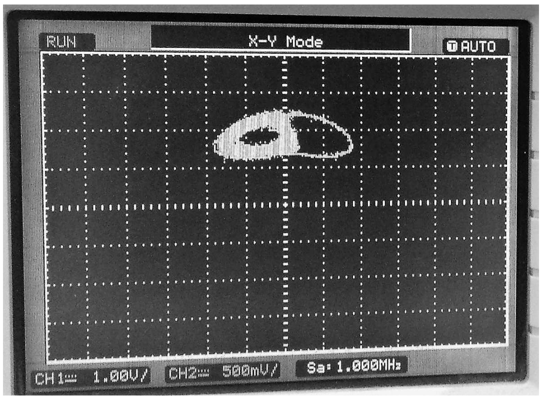

(a) *Oscilloscope trace*

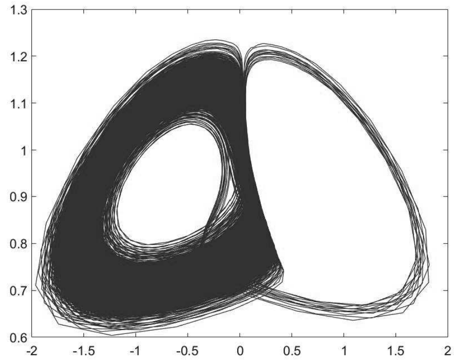

(b) *Acquired waveform*

Figure 4.9: Experimental trend of the attractor on the zy-plane before pellet injection.

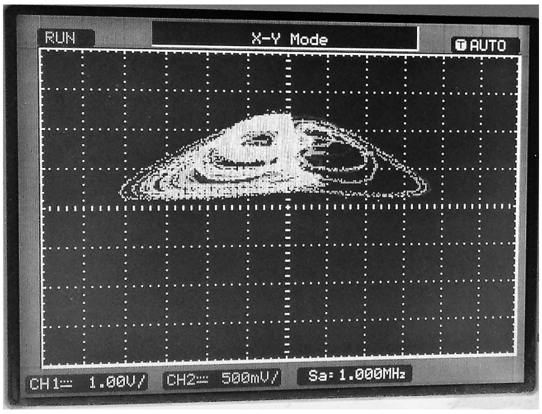

(a) *Oscilloscope trace*

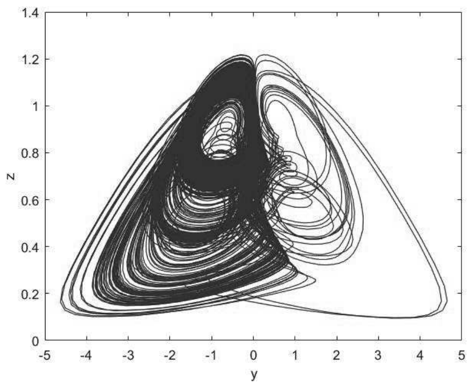

(b) *Acquired waveform*

Figure 4.10: Experimental trend of the attractor on the zy-plane after pellet injection.

By varing the value of the t_{period} in the perturbation expression 4.2 is possible to change the frequency of the signal. For istance in the Fig. 4.11 is shown the case with $t_{period} = 35$:

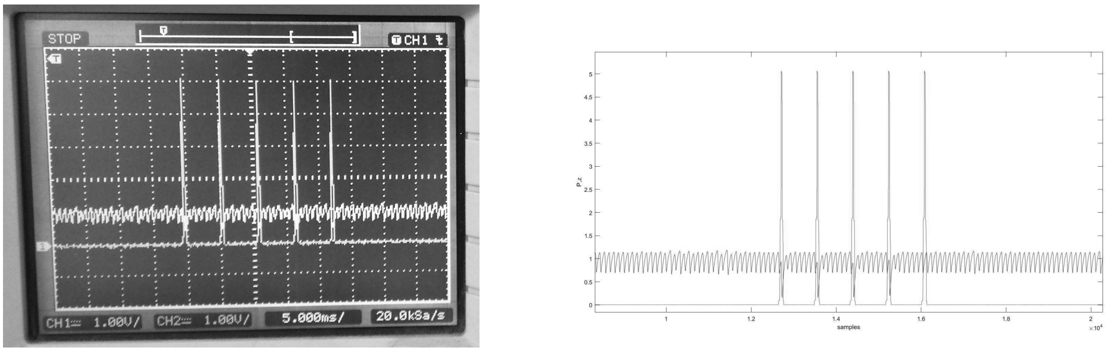

(a) *Oscilloscope trace* (b) *Acquired waveform*

Figure 4.11: Experimental trend of ELMs with pellet injection by varing the parameter t_{period}. Perturbations P(t) are shown by green lines in the case (a) and by red lines in the case (b).

Incresing the t period, the frequency of the perturbation signal decrease thus leading to a more slighter effect on the ELMs.
The **experimental Bifurcation diagram** is built in Matlab®, considering the z variable variation respect the t_{period} parameter:

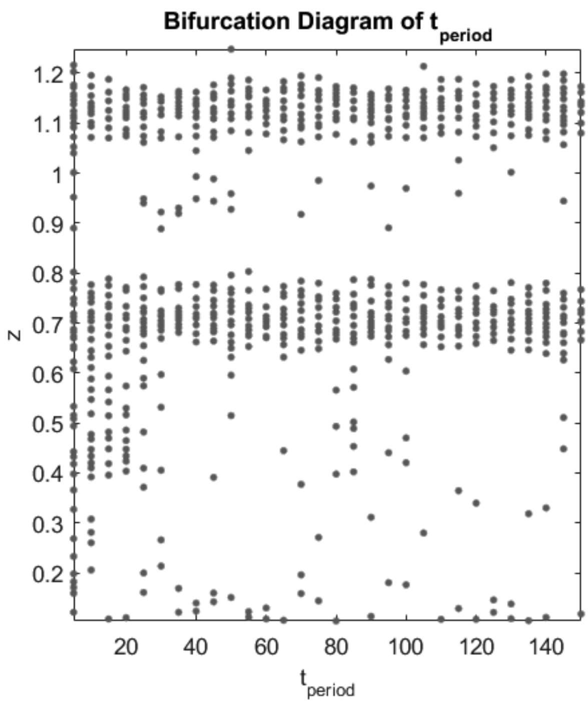

Figure 4.12: Experimental bifurcation diagram with respect to the parameter t_{period}.

From the bifurcation diagram it can be noticed that for higher t_{period} ELMs region is characterized by limit cycle because pellet injection has lower effects on their dynamics. While, for lower t_{period} the system behaves chaotically because the pellet injetion higher affects ELMs thus suppressing them.
As expected the numbers of minimum points decrease with the increase of the t_{period}.

Chapter 5

Conclusions

In this work the proposed **minimal model** examines spatiotemporal phenomena occurring in the vacuum vessel of Tokamaks. The model is a description of the system with drive and relaxation dynamics, which have different time scales.
System dynamic is rather complex. It was described with two equations and by using three parameters (δ, η, h).
Periodic nonlinear perturbation of the plasma result after a certain threshold. The **instability** (Edge Localized Nodes (ELMs), sawteeth) can develop for a critical value of the input power ($h > 1$) and this agrees with experimental observations.
The system behavior for $h = 1.5$ is theoretically explained and then this specific cases are implemented for a practical point of view. The **implementation** was done by using a simple analog nonlinear electronic circuit, that reproduces the real system behavior.
The comparisons bewtween the experimental data and the simulations show a coherence between the two behaviors.
The analysis of the case with **pellet injection** into the plasma was done by using simple electronic components and a low cost microcontroller board Arduino®Uno. The results obtained coincides with the simulations performed in Matlab®. On that basis it is possible to say that the perturbation changes the plasma stability and increases the ELM frequency.
This approach provides a very useful tool for understanding the basic physics of the spatiotemporal evolution of plasma quantities, for detecting the occurance of instabilities and illustrating the possible action of control tecnique.
The **future development** of this work is planned to be the control of the pellet injection with an adaptive law. In this way, when the system behavior is chaotic the t_{period} is kept constant, otherwise in the case of limit cycle, that represent the ELMs condition, the t_{period} is decreased in order to increase the frequency of the pellet.

ISSN: 2278-0181

Bibliography

[1] D. Constantinescu, O. Dumbrajs, V. Igochine, K. Lackner, R. Meyer-Spasche, H. Zohm, and ASDEX Upgrade Team, *A low-dimensional model system for quasi-periodic plasma perturbations. Physics of Plasmas*, 18, 062307, 2011.

[2] Romanelli, F. (2015). *Overview of the JET results.* Nuclear Fusion, 55(10), 104001.

[3] A. Buscarino, C. Corradino, L. Fortuna, *Modeling spatio-temporal complexity during JET instabilities*, IEEE, 2015.

[4] Buscarino, A., Fortuna, L., Frasca, M., & Sciuto, G. (2014). *A concise guide to chaotic electronic circuits.* Springer International Publishing.

[5] Constantinescu, D., Dumbrajs, O., Igochine, V., Lackner, K., Zohm, H., & Team, A. U. (2015). *Bifurcations and fast-slow dynamics in a low-dimensional model for quasi-periodic plasma perturbations.* Romanian Reports in Physics, 67(3), 1049-1060.

[6] Murari, A., Arena, P., Buscarino, A., Fortuna, L., Iachello, M., & JET-EFDA Contributors. (2013). *On the identification of instabilities with neural networks on JET.* Nuclear Instruments and Methods in Physics Research Section A: Accelerators, Spectrometers, Detectors and Associated Equipment, 720, 2-6.

[7] Arduino board, https://www.arduino.cc/.

[8] Arturo Buscarino, Luigi Fortuna, Mattia Frasca, *Essentials of Nonlinear Circuit Dynamics with MATLAB® and Laboratory Experiments*, April 21, 2017 by CRC Press.